FLOW VISUALIZATION EXPERIMENTS ON TETHERED FLYING GREEN LACEWINGS *CHRYSOPA DASYPTERA*

BY DMITRY L. GRODNITSKY AND PAHVEL P. MOROZOV

V. N. Sukachev Institute of Forest and Wood, Siberian Branch of the Russian Academy of Sciences, Krasnoyarsk 660036, Russia

Summary

Experiments on dust visualization of the flow around tethered flying green lacewings showed that, contrary to expectations based on the Weis-Fogh clap-and-fling mechanism, a leading edge separation bubble does not exist near either fore- or hindwings. At the beginning of the stroke cycle each wing operates as an independent generator of vorticity. The vortex bubbles of all the four wings then unite, producing a single U-shaped bubble. A hypothetical spatial structure for the vortex wake is derived from a series of registrated sections of the wake illuminated with a flat light beam. Some problems of wing functional morphology and insect flight aerodynamics are also discussed.

Introduction

Studies of the airflow around flying insects can make an important contribution to the understanding of aerial locomotion. Research in this field is often conducted using artificial models (e.g. Bennett, 1977; Maxworthy, 1979; Savage *et al.* 1979; Spedding and Maxworthy, 1986). Nevertheless, the flow around a mechanical construction and its natural prototype can differ substantially. Aerodynamic investigations of living flying specimens are therefore necessary to verify the effects that have been discovered with models. Also, there are some hypothetical mechanisms of insect flight aerodynamics that need to be corroborated by empirical data. This paper is concerned with some results of flow visualization around flying tethered insects. It must be emphasized that the aerodynamics of tethered flight in still air may differ from that of free flight, so the results must be regarded as tentative.

Materials and methods

Sixteen specimens of the green lacewing *Chrysopa dasyptera* McL. (Neuroptera: Chrysopidae) were collected in the surroundings of Krasnoyarsk City, Middle Siberia, Russia. Experiments were conducted using a modification of the
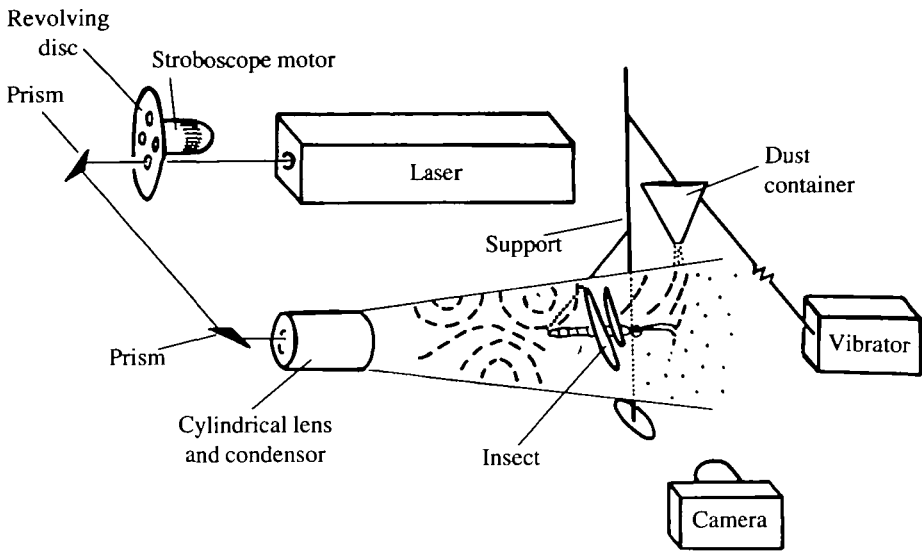
Fig. 1. Diagram of the experimental system.

procedure described by Brodsky and Ivanov (1983, 1984) (Fig. 1). Non-anaesthetized insects were tethered to a pin by the base of their abdomen with the help of Moment-1 glue. The pin was then put on a pivot in front of a camera. Flight was initiated by the tarsal reflex (Fraenkel, 1932) after the support had been removed from under the insect's feet. *Lycopodium* spores served as a visualizing dust. They were released above the flying lacewing from a container shaken by an elastic rod connected to a vibrator. Changing the amplitude of vibration allowed us to regulate the rate of release.

Photographs of visualized flow were taken with a Zenit-19 camera on 35 mm negative A-2 film (light sensitivity 500 ASA). The insect was illuminated with light from a helium–neon laser LG 79–1 (wavelength 633 nm, irradiation power 15 mW). The laser beam passed through the optical system containing a cylindrical lens and formed a strip of light (1 mm thick and 50 mm wide). As all the experiments were conducted in a dark room, the camera registered only the images of those particles that were struck by the light while moving in the plane of the beam. By changing the positions of the camera and the light plane relative to the insect (Fig. 2), we acquired approximately 1000 photographs of the flow around the body and flapping wings in different views at different moments of the stroke cycle. The experimental procedure was as follows. After having acquired photographs with the light beam in position III, the insect was moved a distance equal to a half-span of one wing. Thus, light plane position II was achieved, and photographs of the flow at the midspan of the wings were taken. Photographs of the lateral view near the wing tips were taken when the laser beam occupied position I. The procedure was repeated with the camera in front of the flying insect (Fig. 2B). In an analogous manner, two-dimensional flow photographs were taken
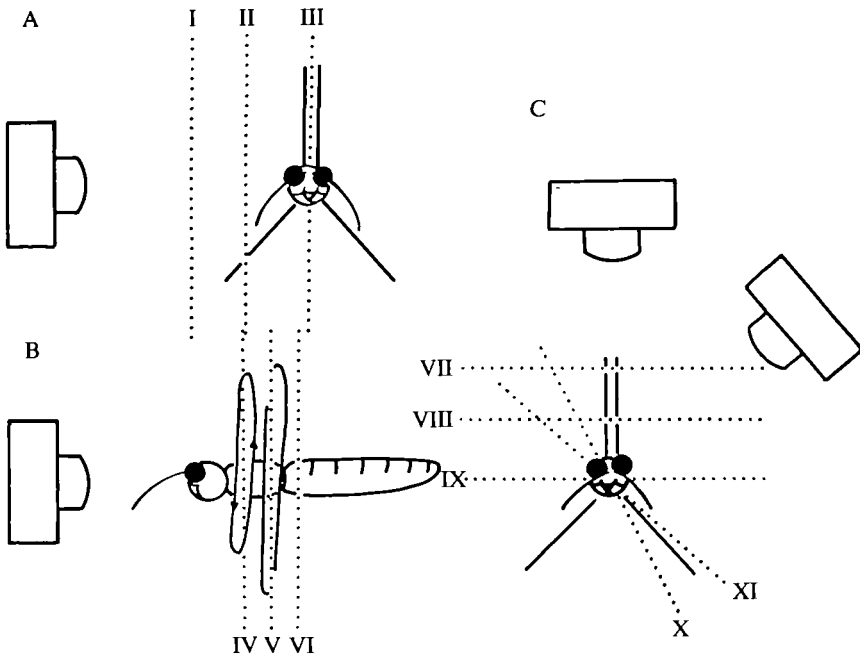
Fig. 2. Positions of camera and light planes relative to the insect. (A) Lateral view (light plane positions I, II, III); (B) frontal view (IV, V, VI); (C) view from above (VII, VIII, IX) and inclined view from the side and above (X, XI).

from above and from the side and above (Fig. 2C). Reconstruction of the three-dimensional structure of the wake was based on this series of two-dimensional pictures. To study the most rapid stroke phases, we used a mechanical stroboscope to interrupt the light beam.

The vortices themselves are invisible on the photographs because dust particles are thrown out of the zone of rapid rotation by centrifugal force. The location of the vortices could only be judged from the direction and shape of micro air streams.

High-speed ciné films of three neuropteran species (*Chrysopa vittata* Wesm., *Kimminsia nervosa* F. and *Hemerobius marginatus* Steph.) performing tethered flight in a wind tunnel with a slow (approximately $0.5 \, \mathrm{m \, s^{-1}}$) air flow were kindly provided by Dr V. D. Ivanov (St Petersburg University).

Results

Kinematics

Analysis of the ciné films showed that the kinematics of the three neuropteran species are quite similar and are in good agreement with our photographic results for *C. dasyptera* and with Ellington's (1984) free flight kinematics for *C. carnea*.
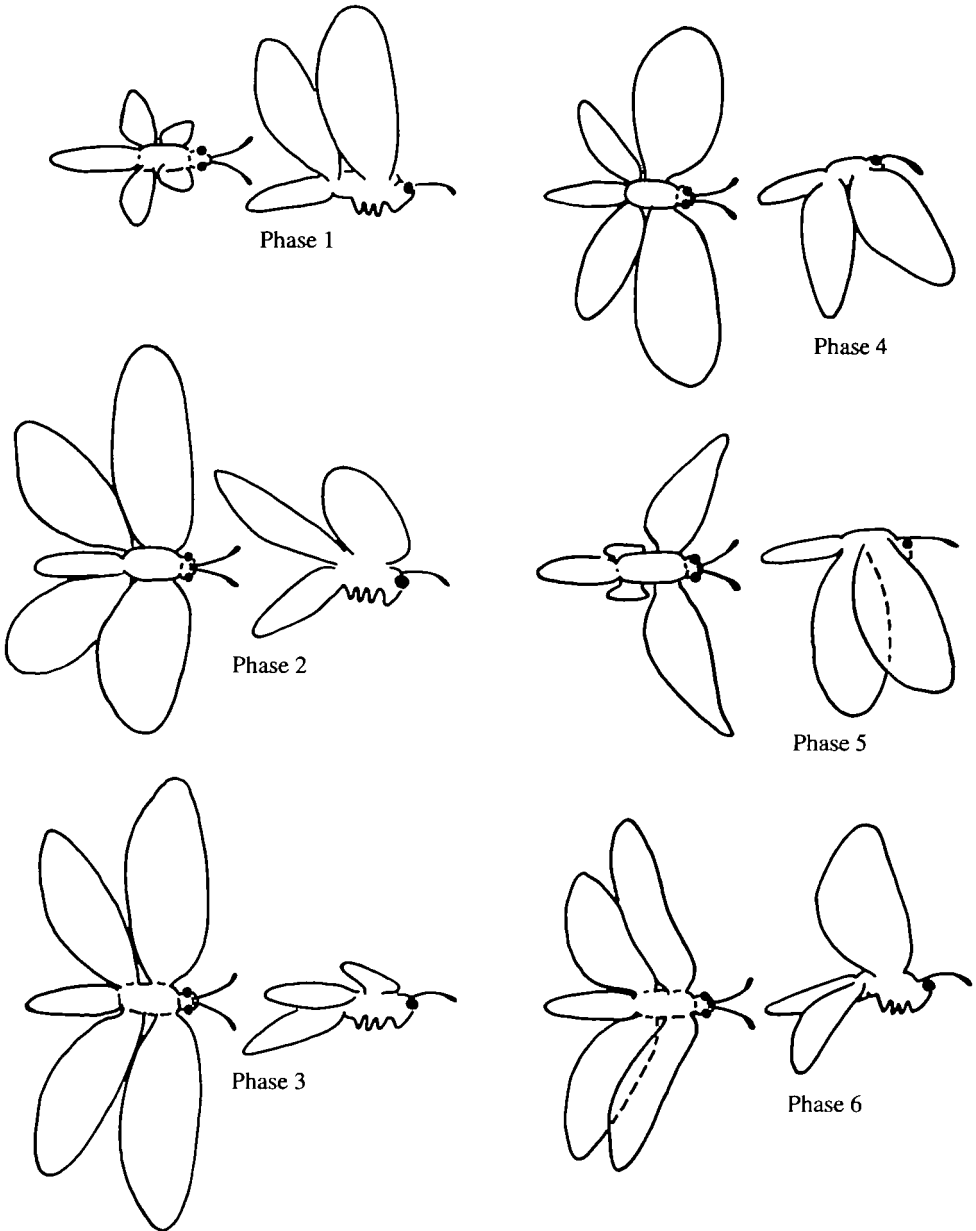
Fig. 3. Wing kinematics illustrated by top and lateral views. The main phases of the stroke cycle are explained in the text.

The main phases of the stroke are shown in Fig. 3. The forewings start their movement slightly earlier than do the hindwings (Fig. 3, phase 1). During the major part of the downstroke fore- and hindwings move together (Fig. 3, phases 2–4). The forewings start to supinate when their positional angle Φ is 120–130°. At

this moment the hindwings are still moving downwards (Fig. 3, phase 5). When the hindwing supination begins at the bottom of their trajectory ($\Phi=170-180°$), the forewings are already moving upwards. During the entire upstroke the two wing pairs flap independently, and the forewings leave the hind ones far behind (Fig. 3, phase 6). In the upper part of the stroke the forewings clap above the body and start the new cycle (Fig. 3, phase 1). The hindwings then do the same, and after that both wing pairs move together again.

Two-dimensional flow visualization

During pronation of the forewings at the very beginning of the downstroke, flow visualization reveals that the air moves smoothly around the leading edges; neither flow reversal nor flow separation was observed (Fig. 4A). Air rushes into the gap between the opening wings without any vortex formation. The vorticity appears later, after the beginning of wing translation. While both wing pairs recede from each other, a clearly visible flow separates from their trailing edges (Fig. 4B) and forms two vortices rotating in opposite directions. This pattern was observed in numerous photographs taken from above with the light plane in positions VII and VIII. As the wings translate, the vortices increase their size (Fig. 4C,D). These cannot be interpreted as tip vortices, which would rotate in the opposite sense (compare Figs 4B and 5B).

During the downstroke, an intensively rotating vortex is observed above the body of the lacewing. This vortex guides the flow back away from the insect (Fig. 5A) and is the 'dorsal' vortex of Brodsky (1988). The flow around the wings is somewhat different and changes with position along the wingspan. A strong 'tip' vortex, which influences the flow across the middle part of the wing, is located directly above the forewing tip (Fig. 5B). Over the wing hinge, the air moves more towards the tip in the general direction of the veins and remigio-anal flexion line. Owing to this slight deflection of air towards the wing tip, a zone of relative deceleration is observed immediately behind the proximal parts of the wings. A characteristic of this phase is considerable weakening or even cessation of the trailing edge flow, so that no vorticity is seen to be shed from the wings.

During supination of the forewings, at the bottom of the downstroke, the tip vortex travels to the tips of the hindwings, which continue with their downward movement (Fig. 6A). Forewing supination changes the relationship between wind velocity under and that above the flapping wing and therefore stimulates a new trailing edge separation of the flow, which deflects downwards (Fig. 6B). After the beginning of the upstroke, this flow curls up to form a vortex that rotates in the opposite direction to that of the dorsal vortex of the downstroke. Thus, a lateral view of the flow at the midspan shows two vortices: the old (upper, dorsal) and new (lower, ventral) ones (Fig. 6C). The subsequent supination of the hindwings is accompanied by the formation of a similar vortex under this pair of wings too (Fig. 6D). While all the four wings move upwards, a single ventral vortex is seen under the insect abdomen (Fig. 7A). A similar picture is seen below the wings
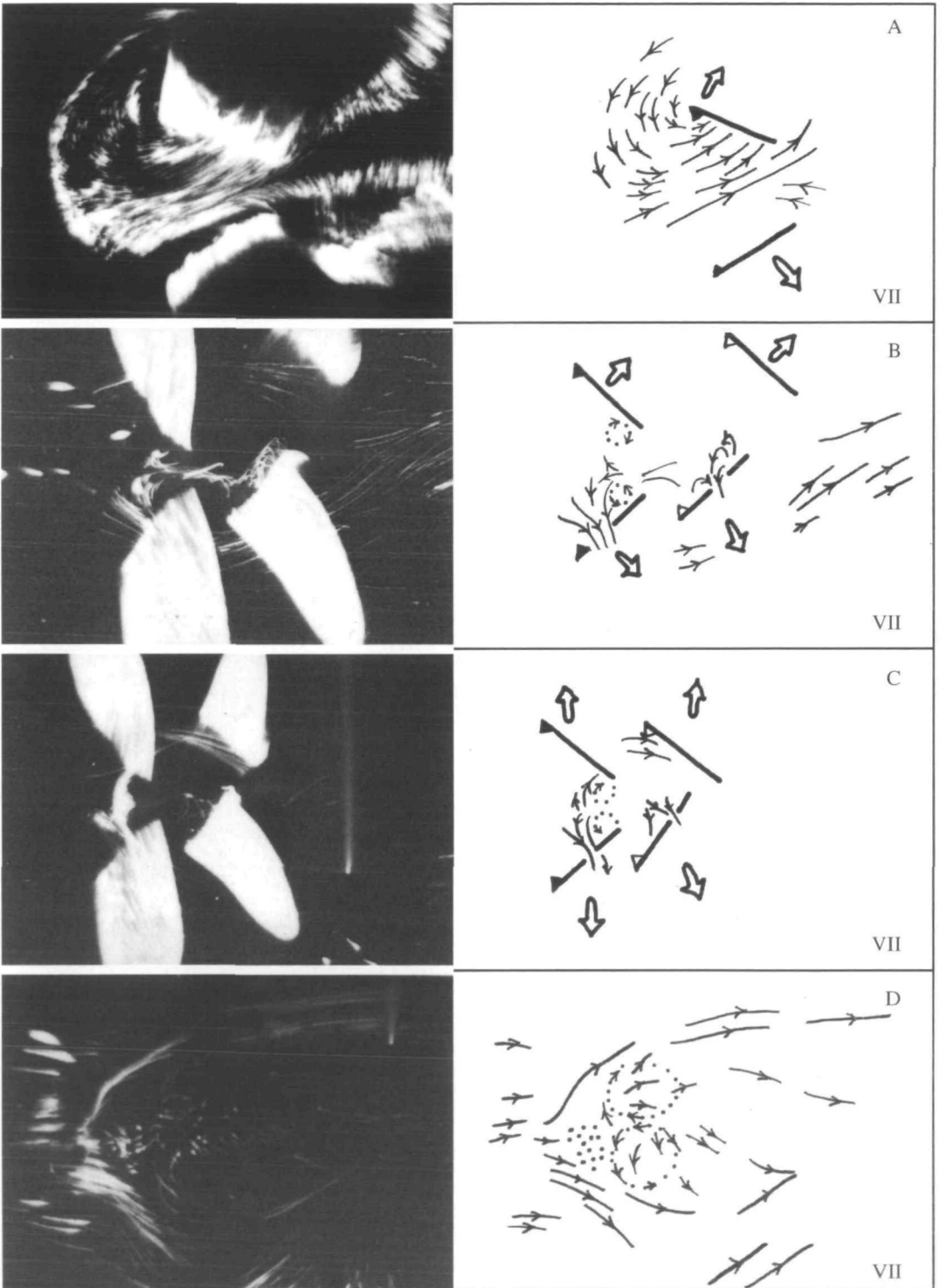
Fig. 4

Fig. 4. Two-dimensional flow around the wings at the beginning of the downstroke (viewed from above, insect facing to the left): kinematic phases 1 (A) and 2 (B–D) (see Fig. 3). Photograph (left) and drawings (right) from them. In this figure and later ones the thin arrows show the direction of air movements, the broad open arrows that of the wings. Circles drawn with a dotted line show the locations of vortices. Triangles mark the upper sides of the leading edges: filled triangles, forewings; open triangles, hindwings. Positions of camera and light plane are labelled with Roman numerals according to Fig. 2. (A) The forewings pronate while the hindwings (not illuminated) move to meet each other; (B) both wing pairs early in the downstroke; (C) the same a bit later; (D) the same, when both fore- and hindwings have gone below the beam plane.
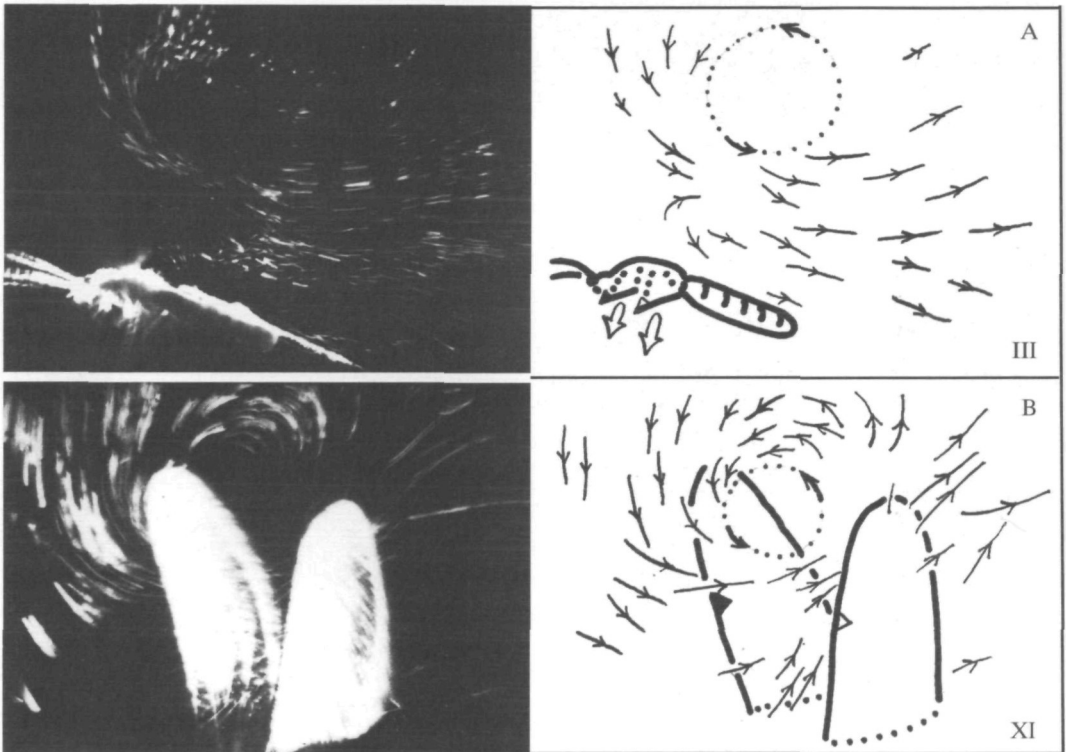

Fig. 5. Two-dimensional flow around the wings and body during the downstroke: phase 3. (A) Dorsal vortex (lateral view); (B) tip vortex on a forewing (inclined view).

(Fig. 7B,C). During the upstroke, the dorsal vortex is located above the lacewing body (Fig. 7A).

The results of the flow visualization show that each wing can operate as an independent generator of vorticity. At the time of wing reversal at either end of the stroke, vorticity is shed independently from fore- and hindwings (Figs 4B and
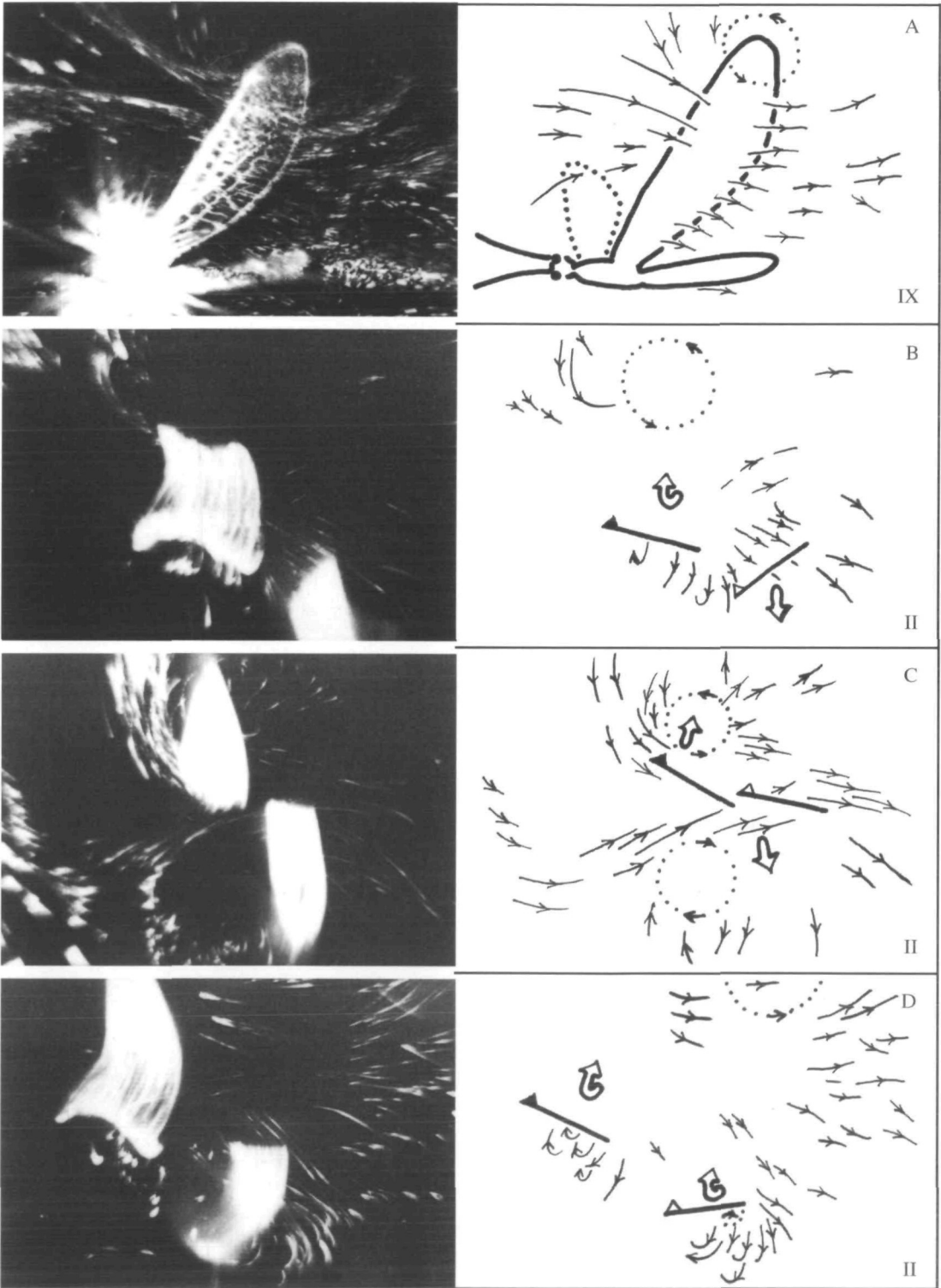
Fig. 6

Fig. 6. Two-dimensional flow around the wings at the bottom of the downstroke: phases 4 and 5. (A) Tip vortex on a hindwing (inclined view); (B) vortex formation under a supinating forewing; (C) a vortex under a forewing moving upwards; (D) vortex formation under a supinating hindwing. Inclined (A) and lateral (B–D) views.
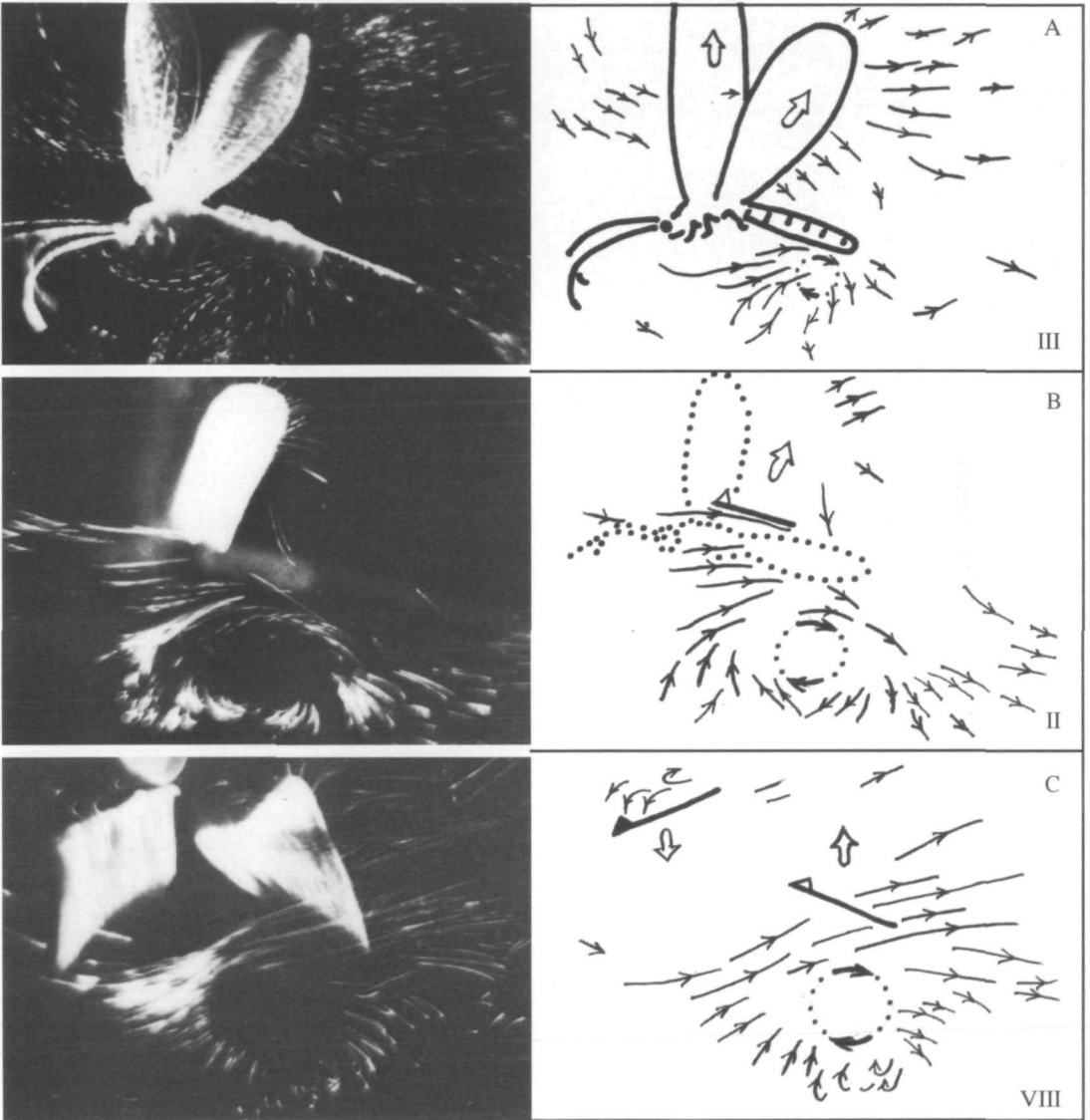

Fig. 7. Two-dimensional flow around the wings and body during the upstroke: phase 6. (A) A vortex under the abdomen; (B) a vortex under a hindwing (lateral view); (C) the same (seen from above).
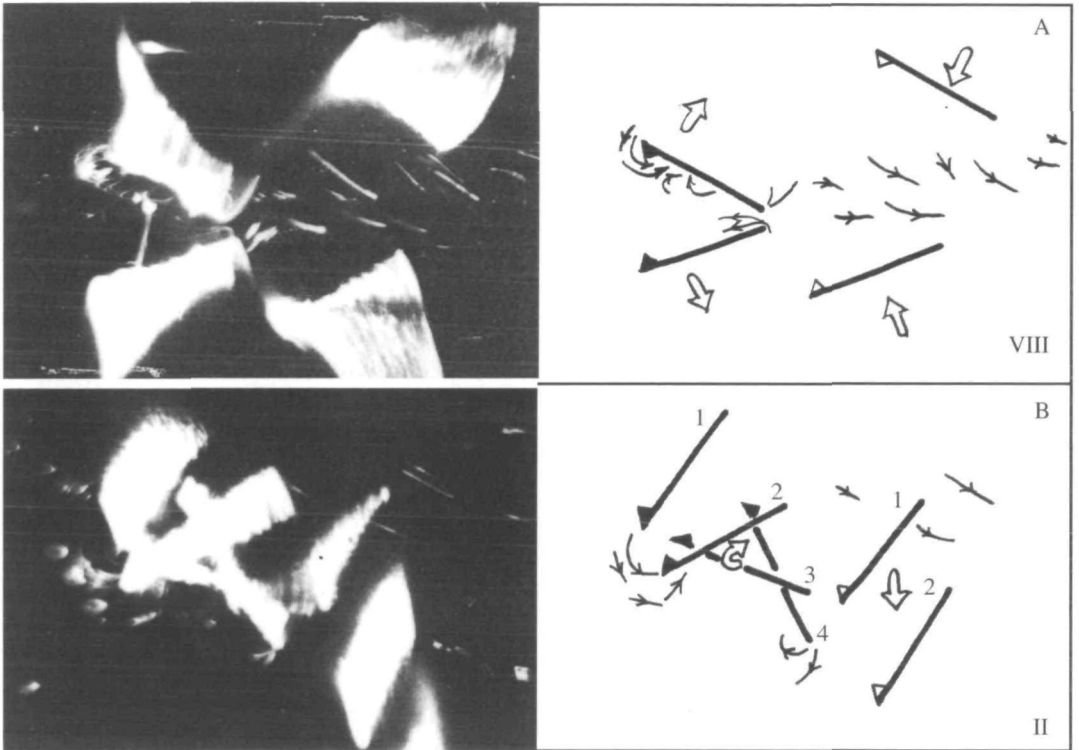
Fig. 8. Separation of the flow from the leading edge of forewings: phases 1 (A) and 5 (B). (A) Pronation at the beginning of a downstroke (seen from above); (B) supination at the bottom of a downstroke (lateral view). The photographs were taken in stroboscopic light (four sequential images near the trailing edge).

6D). As a halfstroke continues, the vortices of the fore- and hindwings are likely to join together, so that only one vortex is observed on each side. This vortex is clearly visible both at the end of the downstroke (Figs 5 and 6A) and in the latter half of the upstroke (Fig. 7). The vortices seem to diminish shedding from the trailing edges of the wings. Such shedding takes place at the beginning of translation for each halfstroke, but disappears as the vortices above and below the wings increase their size. Thus, during most of a halfstroke the airflow comes smoothly off the trailing edges without rotating.

The analysis of photographs, however, reveals that the flow occasionally separates from the leading edge, especially from the forewings at the extreme points of their trajectory (Fig. 8). Nevertheless, this separation has only rarely been observed in photographs of pronating and supinating wings. Moreover, the vortex that must follow such a separation has never been seen; this vortex would have had an opposite sense of rotation to that of the dorsal one. Leading edge separation therefore takes place irregularly and cannot characterize the general

flow around the flapping wings. This phenomenon may also be an experimental artefact resulting from tethered flight in still air.

Reconstruction of the three-dimensional flow

Flat beam illumination, which is fundamental to our experimental procedure, is quite well-known. It was used for the first time in liquid and gas flow studies by Vogel and Feder (1966). More recently it has been applied to investigations of the aerodynamics of flapping models (Maxworthy, 1979; Spedding and Maxworthy, 1986) and living insects (Brodsky and Ivanov, 1983, 1984; Brodsky and Grodnitsky, 1985; Ivanov, 1990). Photographs obtained in these experiments show planar sections of the three-dimensional vortex wake. The complete flow structure is then pieced together from these two-dimensional patterns. The imagination of the scientist is not the least important instrument for this procedure, and interpretation of the two-dimensional results seems to be the main source of contradictions in our understanding of the air movements around flying insects.

At the beginning of each stroke the wing opening causes a non-separating irrotational flow between their dorsal surfaces (Fig. 9A). Some difference in the flow velocity above and below the wing already exists when the trailing edges begin to move apart, causing a discontinuity in the flow shed from the trailing edge. This leads to instability of the flow, and it curls up to form the starting vortex tubes located above the rear part of each wing (Fig. 9B). Every tube is connected to the tip of a wing by a tip vortex (Fig. 5C). As the stroke proceeds, the tubes accumulate the vorticity shed from the wings, increasing their transverse diameter and rotational velocity. Simultaneously, every tube elongates as its proximal end shifts basally. As a result, the tubes coalesce over the body (Fig. 9C), forming a single tube above each wing pair. The tubes from the fore- and hindwings also join together and produce a single U-shaped vortex bubble (Fig. 9D). A sagittal section of this bubble is clearly visible in many photographs (Fig. 5A). Bubble merging may occur early in the downstroke, before the wings reach positional angles of approximately 60°.

The U-shaped bubble is located directly above the body and wings (Fig. 9E) during the whole downstroke. When the forewings approach the lowest point of their trajectory and begin to supinate, the bubble passes to the hindwings, which are still moving downwards (compare Figs 5B and 6A). During this period the U-shaped bubble might prevent flow separation from the trailing edges of both wing pairs.

The beginning of the forewing upstroke is followed by the generation of a vortex bubble which rotates in the opposite sense to that of the U-shaped bubble (Fig. 9F). This is the stopping bubble for the downstroke; at the same time it is a starting vortex for the upstroke. Bubbles on different sides of the body are likely to join together in a manner similar to that in the early stages of the downstroke.

Hindwing supination leads to the formation of an analogous vortex bubble under them (Fig. 9G). Bubbles below hind- and forewings unite at some moment and form a single vortex tube (Fig. 9H); this interpretation is supported by those
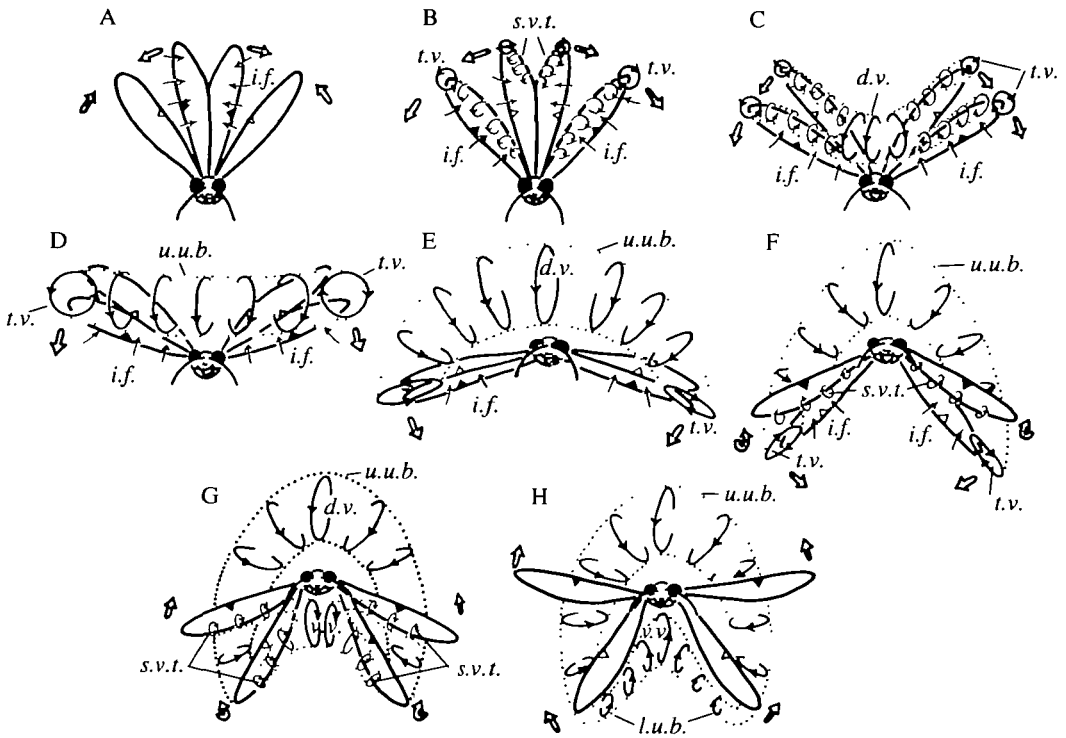
Fig. 9. The hypothetical spatial structure of the flow. Sequential stroke phases: A and B (phase 1) to G and H (phase 6). Viewed from the front. (A) Irrotational flow (*i.f.*) about the leading edge; (B) independent generation of single vortex tubes (*s.v.t.*) above each wing; *t.v.*, tip vortices; (C) start of coalescence of the vortex tubes; *d.v.*, dorsal vortex; (D) formation of the upper U-shaped bubble (*u.u.b.*); (E) growth of the *u.u.b.*; (F) generation of the vortex tubes below the supinating forewings; (G) generation of the vortex tubes below the hindwings and the beginning of the coalescence between single vortex tubes; *v.v.*, the ventral vortex; (H) formation of the lower U-shaped bubble (*l.u.b.*) and birth of a single vortex ring.

flow pictures where only one vortex is seen beneath the body and the wings (Fig. 7). With the beginning of hindwing supination, bubbles underneath and above the insect join to each other through the tip vortices and give birth to a common vortex ring. The shape of this ring differs consistently from toroidal. Viewed from the front, only the upper two-thirds of the ring is visible; the lower third is located below the abdomen, behind the plane containing the wing hinges (Fig. 10A,B). Thus, the formation of the vortex ring resembles the same process in some birds in some flight modes, where the ring consists of starting and stopping bubbles linked to each other (Kokshaysky, 1979).

During the upstroke the ring probably assumes a more regular shape. As the next stroke begins, it is shed from the wings and moves away from the insect (Fig. 10C). As a result, every stroke is followed by the formation of single vortex ring.
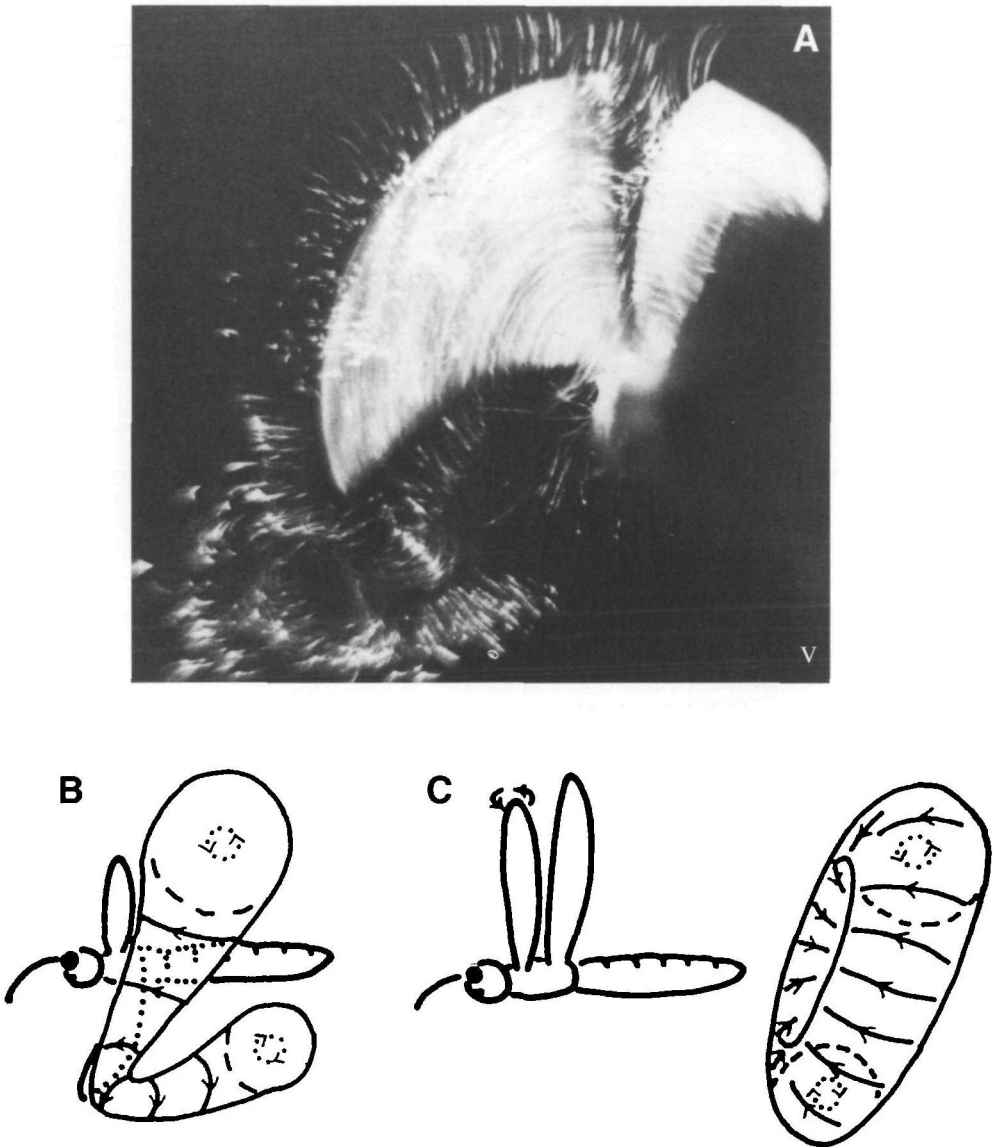
Fig. 10. Overall view of a vortex ring just after its formation (A,B) and after it has lost contact with the wings (C). Viewed from the front (A) and from the side (B,C).

Discussion

According to Weis-Fogh (1973, 1975), wing pronation in the early stages of a stroke plays a role in a special mechanism of lift generation. Weis-Fogh described a book-like opening movement of the wings and called it clap-and-fling. Analysis of this mechanism led Lighthill (1973, 1978) to conclude that clap-and-fling can create a positive force effect in an inviscid fluid without generating any vorticity.

The effectiveness of the mechanism is a robust function of Reynolds number. Lighthill supposed that a useful form may be enhanced in the case of stalling at the leading edge and the subsequent formation of the corresponding vortex bubble. This hypothesis was checked by Belotserkovsky *et al.* (1974), who modelled a two-dimensional flow around a pair of opening wings by the method of discrete vortices. These authors deduced that an insect would gain considerable force if the flow were to separate from the leading edge. Some time later, very similar data were reported by Edwards and Cheng (1982). Maxworthy (1979), in experiments on flow visualization with a flapping mechanical model, confirmed the existence of the leading edge separation bubble. Given this evidence, the majority of authors have had no doubts about the reality of the leading edge flow separation and include it in their schemes of insect flapping flight aerodynamics (Maxworthy, 1981; Ellington, 1984; Wilkin, 1985; Spedding and Maxworthy, 1986; Brodsky, 1988).

Unexpectedly, our results show that after the beginning of a stroke no vorticity is shed from the wings as they rotate about their trailing edges. The air stream moves smoothly around the leading edge and then deflects to the wing tip. Vortex formation is observed only after the wings have started to move apart at the beginning of translation. As this process starts, rotational movement of the air is observed above the trailing edges. Vortices produced in this period cannot be interpreted as leading edge bubbles, since they rotate in the sense opposite to that supposed for the leading edge separation bubble (compare Fig. 4B–D in this paper and Fig. 11 in Maxworthy, 1979). A similar structure from conventional aerodynamics seems to be the starting vortex that develops during the growth of circulation around an aerofoil at the beginning of its movement.

The hypothesis of leading edge separation bubbles probably originated by analogy with work on aircraft. The possibility that the flow separation from a sharp leading edge might have technical applications has been investigated for several decades. For example, it was suggested that this flow separation might improve the lift-to-drag ratio of Concorde and Tu-144 wings (Belotserkovsky and Nisht, 1978) or be useful in the development of vertical take-off and short take-off and landing aircraft (Rossow, 1978). However, this principle has not been fully extrapolated to the aerodynamics of natural flight. A vortex undoubtedly forms at the leading edges of artificial insect wing models fixed in a wind tunnel (Vogel and Feder, 1966; Vogel, 1967) or oscillating in a wind (Savage *et al.* 1979). A similar vortex also forms around flapping mechanical constructions (Maxworthy, 1979, 1981; Spedding and Maxworthy, 1986). However, Rees (1975) observed unseparated flow around a still model of the wing of the hoverfly *Syrphus balteatus*. Moreover, visualization of the flow around detached natural insect wings demonstrates no stalling at the leading edge (Vogel, 1967). A similar conclusion may be derived on the basis of polar curves, which show that increasing the angle of attack does not inevitably result in an abrupt reduction of the lift-to-drag ratio. Thus, it is possible that there is non-separating flow around the wings of a range of insect species: fruit fly *Drosophila virilis* (Vogel, 1967), dragonfly *Aeshna* sp. (Newman *et al.* 1977),

damselfly *Calopteryx splendens* (Rudolph, 1976), crane fly *Tipula oleracea* (Nachtigall, 1977) and various moths and butterflies (Nachtigall, 1967). In the hindwing of *Schistocerca gregaria*, pronounced stalling occurs only under steady-state conditions, whereas the forewings of this species operate without flow separation (Jensen, 1956). Brodsky (1988, 1990) reports the existence of leading edge separation bubbles in living flying insects but does not support his consideration with any experimental data. Visualization of the flow around tethered, flying caddis flies also does not demonstrate separation (Ivanov, 1990).

The smooth flow around natural wings, in contrast to the vorticity generation around mechanical models, is probably due to the presence of microscopic hairs and scales on the wings (Vogel, 1967). A rough calculation using the formula derived for steady-state conditions (Prandtl, 1952, cited in Vogel, 1962) shows that microelements of the wing surface of butterflies and moths do not protrude above the boundary layer and, hence, do not interact with the flow (Grodnitsky *et al.* 1988). Nevertheless, they probably somehow influence the structure of the layer itself (Kokshaysky, 1974) and may, therefore, prevent stalling. The mechanisms of such influences may differ. Hairs and scales may divide the boundary layer into micro streams (Bocharova-Messner, 1982) or induce turbulence in the boundary layer (Kokshaysky, 1974). It is also plausible that micro structures simply serve to increase the area of the wing surface, thus expanding the zone of contact between the boundary layer and a flapping plane. Some effect can be achieved while the air inside the boundary layer decelerates as it passes over the hairs and scales.

Another reason for non-stalling at the leading edge might be provided by a flexible modification of the fling called the peel (Ellington, 1984). According to this hypothesis, the peel is an adaptation for avoiding flow separation from the leading edges of the wings.

The results of our experiments show that stalling and corresponding vortex formation take place near the trailing edges of the wings. This process begins with the start of wing translation at each halfstroke and leads to the formation of a single U-shaped vortex bubble above the insect's body in the downstroke and of another one – below the abdomen – in the upstroke. The parts of this bubble situated close to the wing tips are the tip vortices, whereas its middle parts are the dorsal (above the abdomen) and the ventral (below the abdomen) vortices (Fig. 9). Each time the U-shaped bubble becomes large enough, it begins to prevent stalling from the trailing edges. Hence, the subsequent growth of these vortex structures is probably not due to the shedding of trailing edge vortices, but to the transition of rotating flow from the tip vortices to the dorsal and ventral ones. Thus, during the majority of the stroke cycle the flow close to the wing surface is dominated by the tip vortices with no, or only weak, shedding of vorticity from the trailing edges. This corresponds well to the traditional view of the flow about a flapping wing.

A great deal needs to be done before we solve the problem of the behaviour of flow around insect wings. Nevertheless, the results presented here seem to support the *Kantenschwung-Mechanismus* hypothesis of Nachtigall (1979). A wave-like

motion of the rear part of a wing is thought to enhance a vortex bubble at the beginning of the stroke and subsequently to increase the total lift. There is no contradiction between this mechanism and the non-stalling fling as it was described by Weis-Fogh (1973, 1975) and Lighthill (1973, 1978). Both phenomena can occur, although they will be temporally separated: the swinging edge mechanism follows the clap-and-fling, which occurs at the start of a stroke. Unfortunately, Nachtigall has not described his mechanism in detail, so we are unable to discuss it more thoroughly.

The translocation of the dorsal vortex during the stroke, which has been described in a butterfly (Brodsky and Grodnitsky, 1985) and several caddis flies (Ivanov, 1990), was not found in the green lacewing. This vortex stays in place until almost the very end of the stroke. This discrepancy is rather difficult to explain using available data. It might possibly originate from some undetermined peculiarities of neuropteran wing kinematics.

The spatial model of the vortex wake described here agrees with the experimental data of Ellington (1980), but differs from the earlier hypotheses based on the analysis of dust flow visualizations of tethered, flying insects (Brodsky and Ivanov, 1983, 1984; Brodsky and Grodnitsky, 1985; Ivanov, 1990). According to these authors, the wake of a flying specimen looks like a chain of vortex rings inclined to each other and joined by their upper and lower parts. Each ring is considered to originate during one halfstroke. In contrast, according to our hypothesis, a ring is completely formed only at the end of a downstroke. We have to come to a conclusion that is inconsistent with the earlier proposals because the dorsal vortex that originated in the first halfstroke did not change its location in the second halfstroke. The vortex rings of the down- and upstroke are not spatially separated. The generation of two discrete rings in each stroke is complicated by the pronounced thickness of the vortex tubes and corresponding difficulties of placing them in a rather limited volume around an insect. Moreover, the wings of the species under study do not clap together at the bottom of the trajectory. That is why the rings of the down- and upstroke have a large common part containing up to one-third of a circular axis of each ring. Also, this common part probably promotes the joining together of the vortex structures of different halfstrokes.

The wake shape described here may also result from the inadequacy of experimental conditions, primarily the absence of opposing air flow. The wind from the front might displace the dorsal vortex backwards and, therefore, leave space for the independent formation and closing of the upstroke vortex bubble. As a result, each stroke would be followed by the generation of two vortex rings connected in a V-like manner at their bases (Fig. 11A). Brodsky (1990) came to a similar conclusion on wake structure, having analysed data from smoke visualization of the flow around tethered flying peacock butterfly.

Vortex rings of sequential strokes are not joined to each other. Brodsky (1990) attributes this to the effect of a jet stream which is created, he considers, when the wings clap above the body. In our opinion, jet effects in insect flight are very doubtful, even in species with broad wings (Grodnitsky *et al.* 1988). The jet
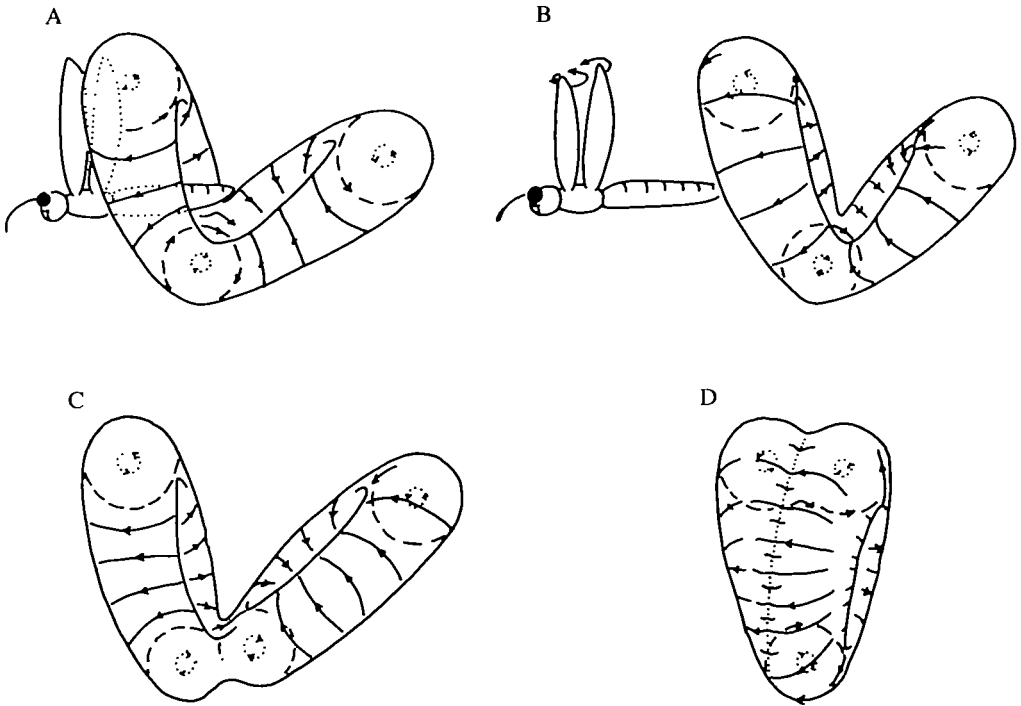
Fig. 11. Possible wake shapes in free flight. Vortices formed during one stroke cycle are shown. (A,B) V-like connected rings before (A) and after (B) they have lost contact with the wings; (C) separating rings; (D) coalescing rings.

phenomenon is even less realistic in lacewings, as their wings are rather narrow. The wake discontinuity is more likely to be due to the fact that the dorsal vortices of the previous and the following strokes are separated spatially and temporally. An 'old' vortex bubble situated between the tips of the wings has to travel down the flow before 'new' vortex tubes will close up and give rise to a new U-shaped vortex bubble located between the proximal halves of the flapping planes.

The stability of such a wake is highly problematic and has not yet been investigated. It is possible that the V-like connected rings coalesce (Fig. 11D) or, just the opposite, separate fully after moving away from an insect (Fig. 11C). In both these cases the resulting wake would look like a sequence of discrete parallel vortex rings, as was assumed in theoretical models of animal flight (Rayner, 1979; Ellington, 1984). In any case, the wake is unlikely to be long. In the photographs, as many as six vortices have been observed at a time, so that the total wake consists of a maximum of three vortex rings. The rotation of air in the wake seems to decelerate quickly under the influence of viscid effects. Thus, vortices dissipate within less than 0.1s.

The fore- and hindwings are not connected and they move with some phase shift during flight. Each wing acts as an independent generator of vorticity at particular

moments of the stroke. Vortex bubbles, which have been produced on different wings, then coalesce. Some deceleration of air rotation might take place at this moment, so that the total lift would be reduced to some extent. This might have been one of the reasons why, during evolution, the insect fore- and hindwings became mechanically connected and united into a single flapping plane. Functionally, two-winged insects may also generate a double dorsal vortex at the beginning of the stroke, but this is an irregular phenomenon taking place only in occasional, rare strokes (Brodsky and Grodnitsky, 1985).

Discussion of the problems of the analytical description of insect flight aeromechanics is beyond the scope of this paper. We would like to note only two important points. A flapping wing operates within near-to-start conditions. Because of this, during a stroke a wing has no time to create the maximum circulation possible for a given wing shape, size and flapping velocity. The compensation of the Wagner effect losses probably results from the constant location of vortices close to the body and the wings. Thus, a flapping plane is influenced by its own wake at almost every moment of its stroke. This phenomenon was first referred to by Savchenko (1971). The interaction of the wings with vortex tubes may considerably change not only the magnitude and the direction of the total force but even the very mechanism of its generation. For example, the presence of a U-shaped vortex bubble above the body and its movement to the wing tips would obviously create a rarefaction and the corresponding lift (Brodsky and Ivanov, 1983, 1984). This is why the insect's body is likely to participate in lift generation, as proposed by Hocking (1953).

From the point of view of processes in the flow around a flapping wing, the total stroke cycle can be subdivided into several phases. Phase 1 is the beginning of the fling (or peel) and is accompanied by pronation of the wing, which stimulates smooth flow above its dorsal surface (Fig. 12A). Phase 2 is the beginning of translation of the wing and is followed by flow separation from the trailing edge, giving rise to a vortex tube that appears to the upper rear of the wing (Fig. 12B). Phase 3 occurs as translation proceeds, the single vortex tube uniting with those above the other wings, forming one U-shaped upper bubble (its sagittal section is the dorsal vortex). The bubble smooths out the flow above the wing, preventing separation from the trailing edge. This phase lasts until the end of the downstroke (Fig. 12C). Phase 4 consists of supination and the beginning of reverse translation of the wing at the start of the upstroke, which cause a new trailing flow separation below the wing. This process results in the development of a single vortex tube beneath the wing surface (Fig. 12D). In phase 5, the single tube coalesces with those of the other wings, forming the lower U-shaped vortex bubble, whose sagittal section is the ventral vortex. This bubble stops stalling at the trailing edge of the wing. Lower and upper bubbles join into one vortex ring, which travels away from the insect after the end of the wing stroke (phase 6). We propose that the different flow patterns occurring at different phases are characterized by different mechanisms of force generation.

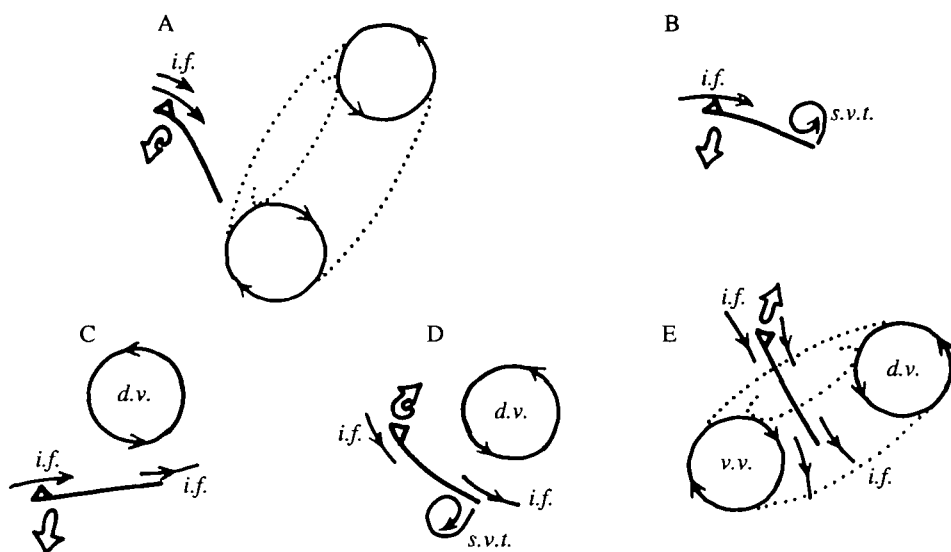The complexity and great instability of the flow around a flying insect make it

Fig. 12. Schematic diagram showing the development of processes in the air flow around a flapping insect wing. Abbreviations as in Fig. 9. For an explanation, see the text.

difficult to interpret the data acquired from visualization experiments. Every new paper dealing with this problem asks new questions but rarely answers old ones. This work is no exception. Thus, the problem of the connection and separation of vortex rings is far from being resolved. The mechanism of the transition of the U-shaped bubble from fore- to hindwings at the bottom of the downstroke is unclear. Practically nothing is known about the quantitative description of the wake. Much more information is needed. We suggest that the most valuable data will be obtained by using different experimental methods, in particular, photography and cinematography in a flat beam, taking stereopairs. Investigation of other insect species, differing in morphology and kinematics, is also highly desirable.

References

BELOTSERKOVSKY, S. M., GULYAYEV, V. V. AND NISHT, M. I. (1974). On the study of flight of insects and birds. *Doklady Akademii Nauk SSSR* **219**, 560–570. (In Russian).

BELOTSERKOVSKY, S. M. AND NISHT, M. I. (1978). Separating and non-separating flow around thin wings in ideal fluid. *Moscow: Nauka Publishing House*. (In Russian).

BENNETT, L. (1977). Clap and fling aerodynamics – an experimental evaluation. *J. exp. Biol.* **69**, 261–272.

BOCHAROVA-MESSNER, O. M. (1982). Insect flapping plane as an example of a morphological model of a life-supplying system. In *Problems of Development of Animal Morphology* (ed. E. I. Vorobyova), pp. 128–139. Moscow: Nauka Publishing House. (In Russian).

BRODSKY, A. K. (1988). *Mechanics of Insect Flight and Evolution of their Flying System.* Leningrad: Leningrad University Press. (In Russian).

BRODSKY, A. K. (1990). Experimental study of flight in peacock butterfly *Inachis io* (Lepidoptera, Nymphalidae). *Zool. Zhurn.* **69**, 39–50. (In Russian).

BRODSKY, A. K. AND GRODNITSKY, D. L. (1985). Aerodynamics of tethered flight of skipper *Thymelicus lineola* Ochs. (Lepidoptera, Hesperiidae). *Entomologicheskoye Obozreniye* **64**, 484–492. (In Russian).

BRODSKY, A. K. AND IVANOV, V. D. (1983). Air flow visualization around a flying insect. *Doklady Akademii Nauk SSSR* **271**, 742–745. (In Russian).

BRODSKY, A. K. AND IVANOV, V. D. (1984). Role of vortices in insect flight. *Zool. Zhurn.* **63**, 197–208. (In Russian).

EDWARDS, R. H. AND CHENG, H. K. (1982). The separation vortex in the Weis-Fogh circulation-generation mechanism. *J. Fluid Mech.* **120**, 463–473.

ELLINGTON, C. P. (1980). Vortices and hovering flight. In *Instationäre Effekte an Schwingenden Tierflügeln* (ed. W. Nachtigall), pp. 64–101. Wiesbaden: F. Steiner.

ELLINGTON, C. P. (1984). The aerodynamics of hovering insect flight. *Phil. Trans. R. Soc. Lond.* B **305**, 1–181.

FRAENKEL, G. (1932). Untersuchungen über die Koordination von Reflexen und automatische-nervösen Rhythmen bei Insekten. I. Die Flugreflex der Insekte und ihre Koordination. *Z. vergl. Physiol.* **16**, 371–393.

GRODNITSKY, D. L., KOZLOV, M. V. AND NESINA, M. V. (1988). The problem of creating of insect flying system well-fitted model. I. A review. *Uspekhi Sovremennoi Biologii* **105**, 284–299. (In Russian).

HOCKING, B. (1953). The intrinsic range and speed of flight of insects. *Phil. Trans. R. Soc. Lond.* **104**, 223–345.

IVANOV, V. D. (1990). A comparative study of flight aerodynamics in caddis flies (Insecta: Trichoptera). *Zool. Zhurn.* **69**, 46–60. (In Russian).

JENSEN, M. (1956). Biology and physics of locust flight. III. The aerodynamics of locust flight. *Phil. Trans. R. Soc. Lond.* B **239**, 511–552.

KOKSHAYSKY, N. V. (1974). *An Essay on Biological Aero and Hydrodynamics.* Moscow: Nauka Publishing House. (In Russian).

KOKSHAYSKY, N. V. (1979). Tracing the wake of a flying bird. *Nature* **279**, 146–148.

LIGHTHILL, M. J. (1973). On the Weis-Fogh mechanism of lift generation. *J. Fluid Mech.* **60**, 1–17.

LIGHTHILL, M. J. (1978). A note on 'clap and fling' aerodynamics. *J. exp. Biol.* **73**, 279–280.

MAXWORTHY, T. (1979). Experiments on the Weis-Fogh mechanism of lift generation by insects in hovering flight. I. Dynamics of the 'fling'. *J. Fluid Mech.* **93**, 47–63.

MAXWORTHY, T. (1981). The fluid dynamics of insect flight. *A. Rev. Fluid Mech.* **13**, 329–350.

NACHTIGALL, W. (1967). Aerodynamische Messungen am Tragflügelsystem segelnder Schmetterlinge. *Z. vergl. Physiol.* **54**, 210–231.

NACHTIGALL, W. (1977). Die aerodynamische Polare des Tipula-Flügels und eine Einrichtung zur halbautomatischen Polarenaufnahme. In *The Physiology of Movement: Biomechanics* (ed. W. Nachtigall), pp. 347–352. Stuttgart: G. Fischer Verlag.

NACHTIGALL, W. (1979). Rasche Richtungsänderungen und Torsionen schwingender Fliegenflügel und Hypothesen über zugeordnete instationäre Strömungseffekte. *J. comp. Physiol.* A **133**, 351–355.

NEWMAN, B. G., SAVAGE, S. B. AND SCHOUELLA, D. (1977). Model tests on a wing section of an *Aeshna* dragonfly. In *Scale Effects in Animal Locomotion* (ed. T. J. Pedley), 445–477. New York: Academic Press.

PRANDTL, L. (1952). *Fluid Dynamics*. New York: Hafner Publishing Co.

RAYNER, J. M. V. (1979). A vortex theory of animal flight. I. The vortex wake of hovering animal. *J. Fluid Mech.* **91**, 697–730.

REES, C. J. (1975). Aerodynamic properties of an insect wing section and a smooth aerofoil compared. *Nature* **258**, 141–142.

ROSSOW, V. J. (1978). Lift enhancement by an externally trapped vortex. *J. Aircraft* **15**, 618–625.

RUDOLPH, R. (1976). Die aerodynamischen Eigenschaften von *Calopteryx splendens* (Harris) (Zygoptera: Calopterygidae). *Odonatologica* **5**, 383–386.

SAVAGE, S. B., NEWMAN, B. G. AND WONG, D. T.-M. (1979). The role of vortices and unsteady effects during the hovering flight of dragonflies. *J. exp. Biol.* **83**, 59–77.

SAVCHENKO, JU. N. (1971). Some peculiarities of hydrodynamics of a flapping wing. *Bionika* **5**, 11–19. (In Russian).

SPEDDING, G. R. AND MAXWORTHY, T. (1986). The generation of circulation and lift in a rigid two-dimensional fling. *J. Fluid Mech.* **165**, 247–272.

VOGEL, S. (1962). A possible role of the boundary layer in insect flight. *Nature* **193**, 1201–1202.

VOGEL, S. (1967). Flight in *Drosophila*. III. Aerodynamic characteristics of fly wings and wing models. *J. exp. Biol.* **46**, 431–443.

VOGEL, S. AND FEDER, N. (1966). Visualization of low-speed flow using suspended plastic particles. *Nature* **209**, 186–187.

WEIS-FOGH, T. (1973). Quick estimates of flight fitness in hovering animals, including novel mechanisms for lift production. *J. exp. Biol.* **59**, 169–230.

WEIS-FOGH, T. (1975). Flapping flight and power in birds and insects, conventional and novel mechanisms. In *Swimming and Flight in Nature*, vol. 2 (ed. T. Y. Wu, C. J. Brokaw and C. Brennen), pp. 729–762. New York: Plenum Press.

WILKIN, P. J. (1985). Aerodynamics. In *Comprehensive Insect Physiology, Biochemistry and Pharmacology*, vol. 5 (ed. G. A. Kerkut and L. J. Gilbert), pp. 553–570. Oxford: Pergamon Press.